

Ionospheric data assimilation: Comparison of extracted parameters using full density profiles and key parameters

Shun-Rong Zhang,¹ William L. Oliver,^{2,3} John M. Holt,¹ and Shoichiro Fukao⁴

Abstract. This paper explores the relative accuracy of deriving solar EUV flux, exospheric temperature T_{ex} , and meridional winds using complete altitude profiles of ionosphere electron density as compared to just using key parameters such as N_{max} , h_{max} and ionospheric electron content. Incoherent scatter radar observations at Millstone Hill and Shigaraki and an ionospheric model are used in this study. We can make the following points: (1) With either the profile or key parameter data, the EUV flux can be inferred with little ambiguity, given that background variables such as the meridional wind are known. (2) The southward wind and T_{ex} can be simultaneously derived from either type of data. The results, in particular the $[\text{O}]/[\text{N}_2]$ results, are similar for the two types of data. The accuracy of the wind result relies much on the accuracy of h_{max} as well as the geomagnetic dip angle. (3) A few key ionospheric parameters are not always sufficient to give a unique definition of ionospheric conditions. Additional parameters or even a full profile data are sometimes needed. In general, however, the key parameter pair h_{max} - N_{max} seems to be a suitable assimilation data source, at least for retrieving the local features of the T_{ex} and meridional wind variation.

1. Introduction

Ionospheric measurements provide diverse types of electron density N_e parameters. The N_e profile data from incoherent scatter (IS) radar gives detailed information about the vertical distribution but there is relatively sparse temporal and geographic coverage. Ionospheric characteristic key parameters (descriptors), such as the peak density N_{max} and its altitude h_{max} and height-integrated ionospheric electron content IEC, are easily measured but do not reflect the complete features of the N_e distribution.

Some assimilation methods have been developed to make use of these data. Assimilation studies first aim at retrieving the basic chemistry and dynamics and then proceed to forecasting ionospheric behavior. The basic idea lies in inserting the data into a first-principles model whose driving forces, such as winds, composition, solar flux, *etc.*, are adjustable. Optimal values of the driving forces are those giving the best match of the model output to the data. In inferring the neutral wind and sometimes the exospheric temperature, previous researchers have assimilated h_{max} [e.g., Miller *et al.*, 1986; Buonsanto *et al.*, 1989; Titheridge, 1993], IEC [Antoniadis, 1977], or both h_{max} and N_{max} [Richards *et al.*, 1998; Zhang *et al.*, 1999; Sojka *et al.*, 2001]. Full electron density profiles have also been applied by Mikhailov and Forster [1997, 1999] and Zhang *et al.* [2001b, 2002]. Such data assimilation methods are subject to ambiguity between the derived variables. First, when can we set

variables to climatology values as approximations to their true status, or how does the use of background variables affect the inferred variables? Second, how is the ambiguity among the variables to be inferred? In partly answering these concerns, Zhang *et al.* [2001b] have assimilated IS radar N_e profile data to examine the uniqueness for paired variables. Then, by considering the ambiguity problems, Zhang *et al.* [2002] have derived a solar EUV flux scaling factor, effective exospheric temperature T_{ex} and meridional winds from the entire N_e profile measured by IS radars.

With this experience in N_e profile assimilation, it is now appropriate to address the accuracy of the use of ionospheric key parameters such as N_{max} , h_{max} , and IEC for determining the information on EUV flux, neutral densities, and winds. The key parameters are being measured constantly with good geographic coverage and are essential for current space weather studies. For instance, the effort to perform assimilation with multiple ionospheric data sources has been under way very actively in a few research groups working on GAIM (Global Assimilation of Ionospheric Measurements) [e.g., Schunk *et al.*, 2002], and the Kalman Filter has been applied to this study [Scherliess, *et al.*, 2002; Hajj *et al.*, 2002]. The ambiguity/uniqueness of inferred variables, however, has yet to be seriously considered in literature. We examine here the differences incurred when one, two, or three key parameters are used. We emphasize here the relative change in our results rather than absolute values, which were discussed by Zhang *et al.* [2002]. We hope our exercises will provide useful information on these ambiguities.

In this study we use a set of N_e data measured by IS radars at Millstone Hill (42.6°N, 288.5°E) and Shigaraki (34.85°N, 136.1°E). We first describe the data, the assimilative ionospheric model and the assimilation method in Section 2, then we compare results from the profile data assimilation with those from the key parameter data assimilation in Section 3, and in Section 4 we discuss results from various combinations of the parameters. Section 5 is our summary.

2. Data, Model and Method

The Millstone Hill IS radar (MHR) and the Shigaraki middle and upper atmosphere radar (MUR) both provide power profile measurements which, to get the N_e profile, are calibrated with ionosonde

¹Haystack Observatory, Massachusetts Institute of Technology, Westford, Massachusetts

²Center for Space Physics, Boston University, Boston, Massachusetts

³Department of Electric and Computer Engineering, Boston University, Boston, Massachusetts

⁴Radio Science Center for Space and Atmosphere, Kyoto University, Kyoto, Japan

N_{\max} and corrected for plasma temperature effects. The N_e data we used have a range resolution of 48 km for the MHR and 9.6 km for the MUR. h_{\max} and IEC (electron content in 220- to 450-km height range) are then found from the N_e profile. Also used is the plasma temperature as input to our assimilative model described below; for the MHR this has a height resolution of 48 km and for the MUR 45 km. Ion drifts were measured by the MHR but not by the MUR for the day we are studying: Day 278 in 1989 when the solar activity was high and geomagnetic activity was low.

Our time-dependent model, originated from *Zhang and Huang* [1995] and *Zhang et al.* [1999], solves the O^+ diffusion equation, derived from the continuity and the momentum equations, and the continuity equations for NO^+ , O_2^+ , and N_2^+ to compute N_e over 100- to 500-km altitude. Plasma temperatures are set to measured data. To allow for the $\mathbf{E} \times \mathbf{B}$ drift contribution to the ion vertical motion, we use the measured meridional ion drift perpendicular to the geomagnetic field for the Millstone Hill computation and an empirical MU radar ion drift model [*Zhang et al.*, 2001a] for the Shigaraki computation.

Neutral composition, temperature, winds and solar flux are the model variables to be inferred. They are obtained by adjustment of their initial (climatology) values to give a best match with the N_e data: the profile or key parameters. We use the mass spectrometer and incoherent scatter (MSIS86) model [*Hedin*, 1987] to generate an initial atmosphere where exosphere temperature T_{ex} is critical in determining the scale height of atmospheric species and thereby affects the neutral composition at all altitudes above the base of the thermosphere. We adjust T_{ex} by a multiplicative factor, f_T . As initial values of the meridional wind, we use, for Millstone Hill, the wind derived from ion drift measurements [see *Vasseur*, 1969 for this traditional wind determination method], and, for Shigaraki, an HWM-like [*Hedin, et al.*, 1991] height-independent horizontal wind model called the MUR HWMU model [*Kawamura et al.*, 2000], developed from ten years of MUR measurements. Adjustments are made by adding a height-independent value, A_w . The solar EUV model for aeronomic calculations (EUVAC) [*Richards et al.*, 1994] is our initial EUV flux specification and is adjusted with a multiplicative factor f_E .

Our variable adjustment and determination to gain the best N_e fit is accomplished with a standard nonlinear least squares fitting algorithm of the type presented by *Bevington and Robinson* [1992]. This also provides estimates of the uncertainties of the variables determined and their interparameter binary correlations. See *Zhang et al.* [2001b] for details about the profile fitting. For the key parameter fitting, the function χ^2 to be minimized takes the following form:

$$\chi^2 = \left[\frac{M_{\max}(f_T, A_w, f_E) - N_{\max}}{\delta N_{\max}} \right]^2 + \left[\frac{H_{\max}(f_T, A_w, f_E) - h_{\max}}{\delta h_{\max}} \right]^2 + \left[\frac{IEC_m(f_T, A_w, f_E) - IEC}{\delta IEC} \right]^2.$$

In the above equation, N_{\max} , h_{\max} and IEC are the measured data and M_{\max} , H_{\max} and IEC_m are the corresponding model values. δN_{\max} , δh_{\max} , and δIEC are the uncertainty of the three key parameters. For this exploratory study, we set $\delta N_{\max} = 10^{10} \text{ m}^{-3}$, $\delta h_{\max} = 1 \text{ km}$, and $\delta IEC = 125 \times 10^{15} \text{ m}^{-2}$, which are very rough estimates of the data uncertainty. The uncertainty for N_{\max} and h_{\max} are relatively small; the uncertainty for IEC is assumed to be slightly large in order to account for the practical condition when a slant Total Electron Content (TEC) measurement, where

longitude and latitude gradients are involved, are inverted into the vertical TEC. Of course, with all three parameters, we can determine 1-3 variables (f_T , f_E and A_w), with two parameters we can determine 1-2 variables, and with one we can determined only one of the variables. We describe below various two-variable fits. The simultaneous determination of three variables (three-variable fit) is desirable but, as discussed by *Zhang et al.* [2001], usually yields binary parameter correlations near unity so that nearly complete ambiguity prevails.

3. The Profile Fit and the Parameter Fit

3.1. EUV Flux

Given that wind speeds are often available from IS radars or climatological models, we have implemented an f_E - f_T adjustment. This 2-variable-search method is good for climatological studies but might be more questionable during highly dynamic or unusual times when drifts are poorly known. Once accurate information on drifts is added into the assimilation, then we can determine the temperature and wind unambiguously. For our present study, since we care about the relative changes of derived variables due to changes of data type, this 2-variable search is suitable whether or not we know the wind accurately.

3.1.1. Profile results and N_{\max} - h_{\max} -IEC results. When adjusting the f_E - f_T pair, as shown in Figure 1 (upper panel), the profile data assimilation (dots) for both sites yields a weak binary correlation in the morning and a strong one near noon; the N_{\max} - h_{\max} -IEC data assimilation yields similar correlation variations (diamonds). Changes in the EUV flux produce proportional changes in O^+ density. Changes in $[O]$ produce proportional changes in $[O^+]$ when the optical depth is small at h_{\max} but not when the optical depth is large. (The accurate calculation of the optical depth for large solar zenith angles may be susceptible to errors because of errors in cross sections and neutral densities). This optical-depth effect yields a large T_{ex} -EUV correlation near noon but a smaller correlation in the morning when the slant path is long. A meaningful EUV flux can be obtained by averaging the hourly f_E , weighted inversely as the variance of the hourly result, for periods of weak EUV- T_{ex} correlations. Table 1 shows f_E values so derived for both sites. The average for the two sites is 0.79 as the profile data are assimilated, and 0.77 as the three parameters are assimilated, indicating agreement for the two types of data.

3.1.2. Profile results and N_{\max} - h_{\max} results. We now drop the IEC data and use only N_{\max} - h_{\max} fitting. This gives EUV- T_{ex} correlations (crosses in the upper panel, Figure 1) similar to what N_{\max} - h_{\max} -IEC fitting gives. The resulting f_E is 0.76, close to the 0.77 given by the N_{\max} - h_{\max} -IEC fitting.

3.1.3. Adjusting the f_E - A_w pair. f_E can be obtained by adjustments of another variable pair, f_E and A_w , assuming that T_{ex} can be set to the MSIS model value. It yields a weak correlation between f_E and A_w (dots in bottom panels) for the profile data and for the N_{\max} - h_{\max} data as well (crosses in bottom panels), but relatively high for the N_{\max} - h_{\max} -IEC data (diamonds in bottom panels). The meridional wind basically alters h_{\max} and consequently the rates of production and recombination of ionization at h_{\max} while the EUV flux affects only the production rate; thereby the f_E - A_w correlation is weak. h_{\max} , being wind sensitive, is contained in the N_{\max} - h_{\max} data set with higher weighting than in the N_{\max} - h_{\max} -IEC data set, which is more ‘‘density-oriented.’’ It is well known that N_{\max} and IEC are highly correlated because the major contribution to IEC comes from near the peak. We therefore see the higher level of the f_E - A_w correlation with the IEC data

added. The f_E value thus derived, however, is associated with the climatology of the MSIS T_{ex} .

3.2. T_{ex} and Meridional Winds

Assuming that the EUV factor is known, T_{ex} and meridional winds can be simultaneously determined. We take the f_E factor to be 0.79, although any reasonable value can be taken for this study emphasizing the relative changes of derived variables. Figure 2 shows the derived T_{ex} (panel (a)) and southward wind (panel (b)) for assimilating N_{max} - h_{max} -IEC data from the MHR. Error bars represent the standard deviation uncertainty. T_{ex} exhibits a depression before noon and the wind shows fluctuations. The large errors at 13 LT result from the high wind- T_{ex} correlation (panel (f)). Panels (c)-(e) display comparisons between the original N_{max} - h_{max} -IEC data (diamonds) and those generated by the model for the best match. The fitting is found to be excellent.

Zhang *et al.* [2002] have shown in detail T_{ex} and meridional wind results from the profile data for the both sites. Here we compare those results to the N_{max} - h_{max} -IEC parameter-fitting results described above. We first examine the wind- T_{ex} correlation coefficient (Figure 3). Both sites give generally small correlation coefficients for fitting either profile data (dots), N_{max} - h_{max} -IEC data (diamonds), or N_{max} - h_{max} data (crosses). There seem no significantly patterned differences among the correlations obtained with the three types of data. A slight increase in T_{ex} generates higher [O] and [N₂] but lower [O]/[N₂], so a denser neutral atmosphere gives rise to higher h_{max} (diffusion less important) through decreasing the O⁺ loss time constant (life-time) and increasing the diffusive time constant, and lower [O]/[N₂] causes lower N_{max} . But a wind change cannot duplicate a T_{ex} change, since a southward wind causes h_{max} and hence N_{max} to increase (a higher N_{max} is a result of a higher h_{max} , where [O]/[N₂] is larger), but no wind change can cause higher h_{max} and lower N_{max} as can T_{ex} .

The inferred T_{ex} and southward wind, together with the 300-km [O]/[N₂] ratio are shown in Figure 4. T_{ex} values at Millstone Hill are basically lower than the MSIS values (solid line) but similar to those given by the energy equation technique [Bauer *et al.*, 1970] in a climatology study by Buonsanto and Pohlman [1998]. An interesting noon (and pre-noon) depression is seen and resembles the one reported by Oliver and Salah [1988] with the MHR data and the Thermospheric General Circulation Model. The Shigaraki T_{ex} does not show a depression around noon and is high in the afternoon, over the MSIS value. For 0800-1000 LT, our results for Shigaraki are similar to those given by Oliver *et al.* [1991], based on the energy equation method for similar geophysical conditions. T_{ex} , the effective exosphere temperature, is rather high at 1300 LT and 1500 LT reaching about 1850°K for reasons not quite clear to us. In fact, the F_2 -layer peak density is largely proportional to the [O]/[N₂] density ratio, because the O⁺ production rate is basically proportional to [O] while its chemical loss coefficient is proportional to the molecular gas density [N₂], so a photochemical equilibrium solution of the electron density around the peak involves the term of [O]/[N₂]. In this sense, the effective exosphere temperature T_{ex} can be regarded essentially as a proxy for affecting the [O]/[N₂] change.

But more meaningful than the absolute values of T_{ex} is the fact that the Shigaraki T_{ex} from the profile data (dots) and from the N_{max} - h_{max} -IEC T_{ex} data (triangles) differ by less than 100°K, and so do the T_{ex} results for Millstone Hill. The [O]/[N₂] ratio differences for the two types of data are small; smaller than the offset from the MSIS ratio.

The meridional wind for Shigaraki is basically around the empirical HWMMU values (solid line), and the profile data-based wind (dots) agrees well with the N_{max} - h_{max} -IEC data-based wind. For

Millstone Hill, both wind estimates deviate from the ion drift-based radar wind (solid line). It is true that that the radar winds are not always accurate when the neutral density assumption is questionable. But to go back to the original data and re-derive a wind every time we make a MSIS density adjustment is a complicated process, and the magnitude of the effect is uncertain. A further study needs to be done to determine the magnitude of its potential effect. In addition to that, several aspects associated with wind effects and our N_e data may lead to the discrepancy between the N_e -based wind and the ion drift-based wind, and between the winds from the profile data and the key parameter data. Millstone Hill has a magnetic dip angle $I \sim 70$ deg thus the neutral wind effect on O⁺ vertical motion is relatively weak due to $\sin I \cos I \sim 0.28$, whereas $\sin I \cos I \sim 0.50$ for Shigaraki with $I \sim 48^\circ$, almost as large as $\sin I \cos I$ can become. Hence N_e and h_{max} are less sensitive to wind changes at Millstone Hill. A significant wind yields a smaller profile change, and our attempt to get wind estimates from either the profile or the parameter data may have incurred large uncertainty. With the 48-km range resolution of Millstone Hill N_e data applied for the present study, the accuracy of results may further worsen. The h_{max} data based on such profiles with coarse height spacing may not be accurate enough to give reliable winds.

3.3. Profile Comparisons

Now that the derived T_{ex} values from the two types of data are in general agreement, and so are the winds, it is necessary to check if the calculated N_e profiles agree with each other and with the original experimental profile. Three profiles are plotted for each of several hours for Millstone Hill in Figure 5. The solid line represents the calculated profile based on assimilating N_{max} - h_{max} -IEC data, and the dashed line represents the calculated profile based on assimilating the profile data represented by circles. For most times, agreements are seen for the three profiles. This is not surprising because the model driving forces (variables) derived do not differ significantly. However, there are cases, e.g., at 1400 and 1600 LT, when the profile assimilation (dashed line) reproduces well the original profile data (circles), while the parameter assimilation reproduces (solid line) well the original N_{max} - h_{max} -IEC data but not the full profile data. At these times, either T_{ex} values or winds from the two types of data show departures too (see Figure 4).

This kind of ambiguity implies that the same set of key parameters could pertain to different N_e profiles corresponding different atmospheric conditions, and only two or three parameters is sometimes insufficient to give a unique definition of the ionospheric conditions even for the F_2 region. When this happens, other assimilation methods or additional data should be considered. On the other hand, it is often desired for a physical model to reproduce the entire N_e profile through fitting only key parameters N_{max} and h_{max} and having the correct plasma temperatures. Indeed, for the N_e profile well above the F_2 peak, if N_{max} , h_{max} are forced to follow observations by adjusting the solar EUV flux, neutral composition, and meridional wind, and plasma temperatures are set to observations, then the physics of the profile should be well determined, since the EUV flux and [O]/[N₂] effects and the wind effects have been simply represented by, individually, N_{max} and h_{max} , and the profile shape is associated with diffusion effects influenced by the plasma temperatures.

The shape of the N_e profile around and below the peak, however, does not depend on variations of the EUV flux, [O]/[N₂] and wind in a simple manner. It particularly depends on diffusion and chemical loss processes, for which the height distribution of atomic and molecular densities and the neutral temperature are important. Therefore additional N_e data (other than the parameters) should be

supplied for inferring unambiguously the complete physics of the profile. For some particular conditions, disadvantages of using peak parameters may become a problem, e.g., N_e sometimes varies little with altitude around h_{\max} such that the “peak” height is either hard to locate or loses its practical meaning; there are occasions (disturbed periods and summer conditions) when O^+ may be depleted to an extent that the N_{\max} occurs at the peak of the lower-altitude molecular-ion layer; when an empirical method of deducing h_{\max} from the M3000F2 factor is applied, convenient for handling a large volume of historic data, it leads to an inherent uncertainty of 20-25 km, on average.

4. Various Key Parameter Fits

It is also desired to infer atmospheric information from certain ionospheric data, for example, to obtain winds from h_{\max} and to obtain T_{ex} from N_{\max} or IEC. It is in particular the case when data availability is limited for ionospheric data assimilation studies. Here we investigate, in order to obtain one specific variable (T_{ex} or wind), which key parameter (N_{\max} , h_{\max} or IEC) or key parameter combination yields the best results. We compare the parameter-based variable to the profile-based one for examining the goodness of results. As samples of this effort, Figure 6 shows the results for inferring T_{ex} at Millstone Hill and Figure 7 for inferring southward winds at Shigaraki. Tables 2-4 summarize the deviations from the profile data-based parameters. We see that certain parameters or their combinations deviate substantially from the profile result.

4.1. T_{ex} and $[O]/[N_2]$

Table 2 gives the daytime average deviation of T_{ex} in percentage, defined as $100 \times |1 - T_{\text{ex}}(\text{parameters})/T_{\text{ex}}(\text{profile})|$. For Millstone Hill, there appears significant deviation (41%) for IEC, which contains electron density information over a wide height range but in a height-integrated sense. For N_{\max} , the deviation is 13%; adding h_{\max} makes little difference (from 13% to 12% for Millstone). This is not the case for Shigaraki where there appears 20% or 17% deviations for N_{\max} or IEC, and adding h_{\max} to N_{\max} causes a significant reduction of the deviation (to 6%), suggesting the importance of the h_{\max} data for Shigaraki’s assimilation.

The balance height (h_b) between the chemical loss and diffusion, which the F_2 peak height is located around, depends on the geomagnetic dip angle I because the diffusion velocity is proportional to $\sin^2 I$. In fact, $h_b \sim \beta/(d \sin^2 I)$ where β and d are O^+ loss frequency and diffusion coefficient. At Millstone Hill, $\sin^2 I \sim 0.91$ and at Shigaraki, $\sin^2 I \sim 0.55$. Therefore, the same rate of changes in the ratio β/d as a result of T_{ex} modifications will give rise to larger h_{\max} changes at Shigaraki than at Millstone Hill, or we can say h_{\max} is more sensitive to T_{ex} changes at Shigaraki. In general, the data set N_{\max} - h_{\max} provides T_{ex} values with a fairly good accuracy (small deviation), and adding IEC data does not seem to improve the accuracy much. Table 3 shows the $[O]/[N_2]$ ratio results, similar to those in Table 2. Again, the data set N_{\max} - h_{\max} provides reasonable accuracy.

4.2. Winds

Table 4 is for the daytime average deviation of southward winds (not the percentage but the absolute deviation defined as $|\text{Wind}(\text{parameters}) - \text{Wind}(\text{profile})|$). Inferring winds from h_{\max} data alone contains 35 m s^{-1} error for Millstone Hill and 15 m s^{-1} for Shigaraki. The greater deviation at Millstone Hill is due to the larger dip angle, which yields smaller $\sin I \cos I$ for inducing vertical motion of ionization, so that the meridional wind can not be so easily tracked as it can be for Shigaraki by the N_e variations. The 25 m s^{-1} average over both sites can be reduced to 16 m s^{-1} by adding N_{\max} data.

5. Discussion

The accuracy of the absolute values of derived variables is a problem beyond the scope of this work. As stated by Zhang *et al.* [2002], the inferred T_{ex} is essentially a proxy for affecting the $[O]/[N_2]$ change since N_e near the F_2 peak is proportional to the $[O]/[N_2]$ ratio during the daytime. If factors other than thermal expansion have caused $[O]/[N_2]$ to change, our T_{ex} becomes an “effective” exospheric temperature, of reduced physical significance, whereas the $[O]/[N_2]$ ratio is still meaningful. Our T_{ex} tends to be very low around noon at Millstone Hill and high in the afternoon at Shigaraki, suggesting that other factors have indeed affected $[O]/[N_2]$ and our results at these times may not be considered as a true estimate of the exosphere temperature. The accuracy of the data and the assimilative model need also to be taken into account. Although the physics and chemistry are relatively simple during the day for the O^+ dominant regime, modeling errors due to effects of vibrationally excited N_2 and O_2 , and in photoelectron production, cross sections and reaction rates may bias our results.

As stated before, our EUVAC modification factor f_E of 0.79 has been obtained from the 2-variable (f_E - f_T) search with the third variable (meridional winds) set by a climatological model and not adjusted. Such f_E depends generally on the validity of the third variable, although we do see weak binary correlations between f_E and winds, the third variable, as indicated in Section 3.1.3. Using this f_E , we obtain neutral winds in the A_w - f_T search (Section 3.2). This wind result is more than just a noisy version of the assumed climatological winds, because our 0.79 factor is an optimal value obtained by considering the individual f_E as well as the fitting error information for each hour.

In spite of the uncertainty for deriving absolute values of the variables, our conclusions made for the relative changes of the variables in response to changes in the data type, from the profile points to various key parameters, are still valid.

6. Conclusion

Assimilation of incoherent scatter radar electron density data from Millstone Hill and Shigaraki into an ionospheric model has been performed to infer the solar flux, effective exospheric temperature T_{ex} ($[O]/[N_2]$), and meridional wind. These ionospheric model variables are adjusted to give best match of the model N_e to the data. We explore the relative accuracy of deriving these three variables using complete altitude profiles of the ionospheric electron density as compared to just using key parameters of the ionospheric peak (N_{\max} and h_{\max}) and of the ionospheric F layer electron content (IEC). We find that:

1. With either the profile or key parameter data, the EUV flux can be inferred with little ambiguity, given that background variables such as the meridional wind are known.
2. The southward wind and T_{ex} can be simultaneously derived from either type of data. The results, in particular the $[O]/[N_2]$ results, are similar for the two types of data. The accuracy of the wind result relies much on the accuracy of h_{\max} as well as the geomagnetic dip angle.
3. A few key ionospheric parameters are not always sufficient to give a unique definition of ionospheric conditions. Additional parameters or even a full profile data are sometimes needed. In general, however, the key parameter pair h_{\max} - N_{\max} seems to be a suitable assimilation data source, at least for retrieving the local features of the T_{ex} and meridional wind variation.

Acknowledgments. The Millstone Hill incoherent scatter radar is supported by a cooperative agreement between the NSF and Massachusetts Institute of Technology. The MU radar belongs to and is operated by the Radio Science Center for Space and Atmosphere (RASC) of Kyoto University. This work was partly supported by NSF grant through ATM-9700162.

References

- Antoniadis, D. A., Determination of thermospheric quantities from simple ionospheric observations using numerical simulation, *J. Atmos. Terr. Phys.*, **39**, 531-537, 1977.
- Bauer, P., P. Waldteufel, and D. Alcayde, Diurnal variations of the atomic oxygen density and temperature determined from incoherent scatter measurements in the ionospheric F region, *J. Geophys. Res.*, **75**, 4825-4832, 1970.
- Bevington, P. R., and D. K. Robinson, Data Reduction and Error Analysis for the Physical Sciences, 2nd ed., McGraw-Hill, New York, 1992.
- Buonsanto, M. J., J. E. Salah, K. L. Miller, W. L. Oliver, R. G. Burnside, and P. G. Richards, Observations of neutral circulation at mid-latitude during the equinox transition study, *J. Geophys. Res.*, **94**, 987-997, 1989.
- Buonsanto, M. J., and L. M. Pohlman, Climatology of neutral exospheric temperature above Millstone Hill, *J. Geophys. Res.*, **103**, 23,381-23,392, 1998.
- Mikhailov, A. V., and M. Forster, Self-consistent modelling of the daytime electron density profile in the ionospheric F region, *Ann. Geophys.*, **15**, 314-326, 1997.
- Mikhailov, A. V., and M. Forster, Some F2-layer effects during the January 06-11, 1997 CEDAR storm period as observed with the Millstone Hill incoherent scatter facility, *J. Atmos. Sol.-Terr. Phys.*, **61**, 249-261, 1999.
- Hedin, A. E., MSIS-86 thermospheric model, *J. Geophys. Res.*, **92**, 4649-4662, 1987.
- Hedin, A. E., M. A. Biondi, R. G. Burnside, G. Hernandez, R. M. Johnson, T. L. Kileen, C. Mazaudier, J. W. Meriwether, J. E. Salah, R. J. Sica, R. W. Smith, N. W. Spencer, V. B. Wickwar and T. S. Viridi, Revised globe model of thermospheric winds using satellite and ground-based observations, *J. Geophys. Res.*, **96**, 7657-7688, 1991.
- Hajj, G. A., B. D. Wilson, C. Wang, and X. Pi, Ionospheric data assimilation by use of the Kalman Filter, in *10th International Ionospheric effects symposium*, edited by J. M. Goodman et al., pp.231-238, JMG Associates, Ltd., 2002.
- Kawamura, S., Y. Otsuka, S.-R. Zhang, S. Fukao, and W. L. Oliver, A climatology of middle and upper atmosphere radar observations of thermospheric winds, *J. Geophys. Res.*, **105**, 12,777-12,788, 2000.
- Miller, K. L., D. T. Torr, and P. G. Richards, Meridional winds in the thermosphere derived from measurements of layer height, *J. Geophys. Res.*, **91**, 4531-4535, 1986.
- Oliver, W. L., and J. E. Salah, The global thermospheric mapping study, *J. Geophys. Res.*, **93**, 4039-4059, 1988.
- Oliver, W. L., T. Takami, S. Fukao, T. Sato, M. Yamamoto, T. Tsuda, T. Nakamura, and S. Kato, Measurements of ionospheric and thermospheric temperatures and densities with the middle and upper atmosphere radar, *J. Geophys. Res.*, **96**, 17,827-17,838, 1991.
- Richards, P. G., J. A. Fennelly, and D. G. Torr, EUVAC: A solar EUV flux model for aeronomic calculations, *J. Geophys. Res.*, **99**, 8981-8992, 1994.
- Richards, P. G., P. L. Dyson, T. P. Davies, M. L. Parkinson, and A. J. Reeves, Behavior of the ionosphere and thermosphere at a southern midlatitude station during magnetic storms in early March 1995, *J. Geophys. Res.*, **103**, 26,421-26,432, 1998.
- Scherliess, L., R. W. Schunk, J. J. Sojka, and D. C. Thompson, Development of a physics-based reduced state Kalman Filter for the ionosphere, in *10th International Ionospheric effects symposium*, edited by J. M. Goodman et al., pp.210-221, JMG Associates, Ltd., 2002.
- Schunk, R. W., L. Scherliess, J. J. Sojka, D. C. Thompson, D. N. Anderson, M. Codrescu, C. Minter, T. J. Fuller-Rower, R. A. Heelis, M. Hariston, and B. M. Howe, Global Assimilation of Ionospheric Measurements (GAIM), in *10th International Ionospheric effects symposium*, edited by J. M. Goodman et al., pp.50-61, JMG Associates, Ltd., 2002.
- Sojka, J. J., D. C. Thompson, R. W. Schunk, T. W. Bullett, and J. J. Makela, Assimilation Ionosphere Model: Development and testing with Combined Ionospheric Campaign Caribbean measurements, *Radio Sci.*, **36**, 247-259, 2001.
- Titheridge, J. E., Atmospheric winds calculated from diurnal changes in the mid-latitude ionosphere, *J. Atmos. Terr. Phys.*, **55**, 1637-1659, 1993.
- Vasseur, G., Dynamics of the F-region observed with Thomson-scatter-I Atmospheric circulation and neutral winds, *J. Atmos. Terr. Phys.*, **31**, 397-420, 1969.
- Zhang, S.-R., and X.-Y. Huang, A numerical study of ionospheric profiles for mid-latitudes, *Ann. Geophys.*, **13**, 551-557, 1995.
- Zhang, S.-R., S. Fukao, and W. L. Oliver, Data modeling and assimilation studies with the MU radar, *J. Atmos. Sol. Terr. Phys.*, **61**, 563-583, 1999.
- Zhang, S.-R., W. L. Oliver, and S. Fukao, MU radar ion drift model, *Adv. Space Res.*, **27**, 115-120, 2001a.
- Zhang, S.-R., W. L. Oliver, S. Fukao, and S. Kawamura, Extraction of solar and thermospheric information from the ionospheric electron density profile, *J. Geophys. Res.*, **106**, 12,821-12,836, 2001b.
- Zhang, S.-R., W. L. Oliver, J. M. Holt, and S. Fukao, Solar EUV Flux, Exospheric Temperature and Thermospheric Wind Inferred from Incoherent Scatter Measurements of Electron Density Profile at Millstone Hill and Shigaraki, *Geophys. Res. Lett.*, **29**(8), doi:10.1029/2002GL014678, 2002.

S. Fukao, Radio Science Center for Space and Atmosphere, Kyoto University, Uji, Kyoto 611-0011, Japan. (fukao@kurasc.kyoto-u.ac.jp)

J. M. Holt, Haystack Observatory, Massachusetts Institute of Technology, Route 40, Westford, MA 01886. (jmh@haystack.mit.edu)

W. L. Oliver, Department of Electrical and Computer Engineering, Boston University, 8 Saint Mary's Street, Boston, MA 02215. (wlo@bu.edu)

S.-R. Zhang, Haystack Observatory, Massachusetts Institute of Technology, Route 40, Westford, MA 01886. (shunrong@haystack.mit.edu)

(Received 2002; revised 2002; accepted 2002.)

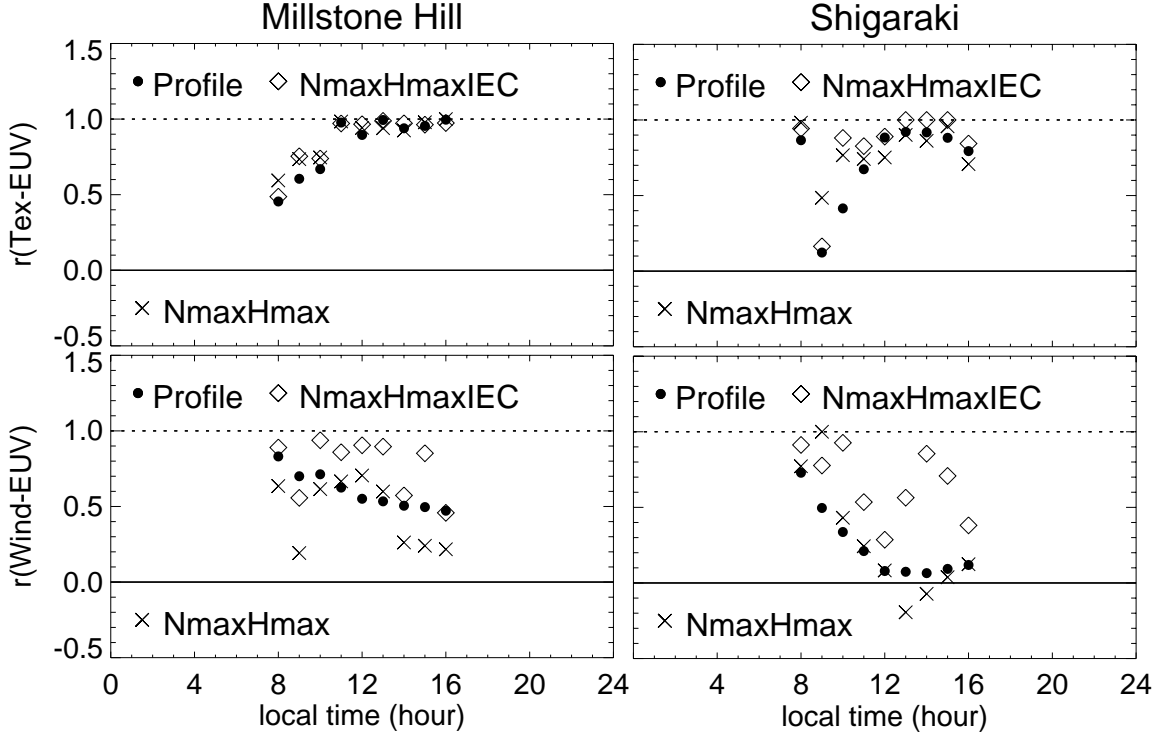


Figure 1. The uniqueness of the inferred EUV flux. Left panels are for Millstone Hill and the right for Shigaraki. Top panels are for T_{ex} -EUV correlation coefficients and the bottom for Wind-EUV. Dots are obtained with the profile assimilation, diamonds with $N_{\text{max}}-h_{\text{max}}$ -IEC data, and crosses with $N_{\text{max}}-h_{\text{max}}$ data.

Table 1. EUVAC Factor f_E for Different Assimilation Data Sets

Data	Millstone	Shigaraki	Average
profile	0.80	0.78	0.79
$N_{\text{max}}-h_{\text{max}}$ -IEC	0.78	0.75	0.77
$N_{\text{max}}-h_{\text{max}}$	0.77	0.75	0.76

Table 2. Percentage Deviations of Inferred T_{ex} from N_{max} , h_{max} and IEC to Those from the N_e Profile^a

^a Values are daytime averages.

Data	Millstone	Shigaraki	Average
$N_{\text{max}}-h_{\text{max}}$ -IEC	9	5	7
$N_{\text{max}}-h_{\text{max}}$	12	6	9
N_{max}	13	20	17
IEC	41	17	29

Table 3. Percentage Deviations of Inferred 300-km $[O]/[N_2]$ from N_{max} , h_{max} and IEC to Those from the N_e Profile^a

^a Values are daytime averages.

Data	Millstone	Shigaraki	Average
$N_{\text{max}}-h_{\text{max}}$ -IEC	11	6	9
$N_{\text{max}}-h_{\text{max}}$	13	6	10
N_{max}	14	17	16
IEC	28	13	21

Table 4. Absolute Deviations of Winds from N_{max} , h_{max} and IEC to Those from the N_e Profile^a

^a Values are daytime averages in unit of m s^{-1} .

Data	Millstone	Shigaraki	Average
$N_{\text{max}}-h_{\text{max}}$ -IEC	17	25	22
$N_{\text{max}}-h_{\text{max}}$	22	10	16
h_{max}	35	15	25

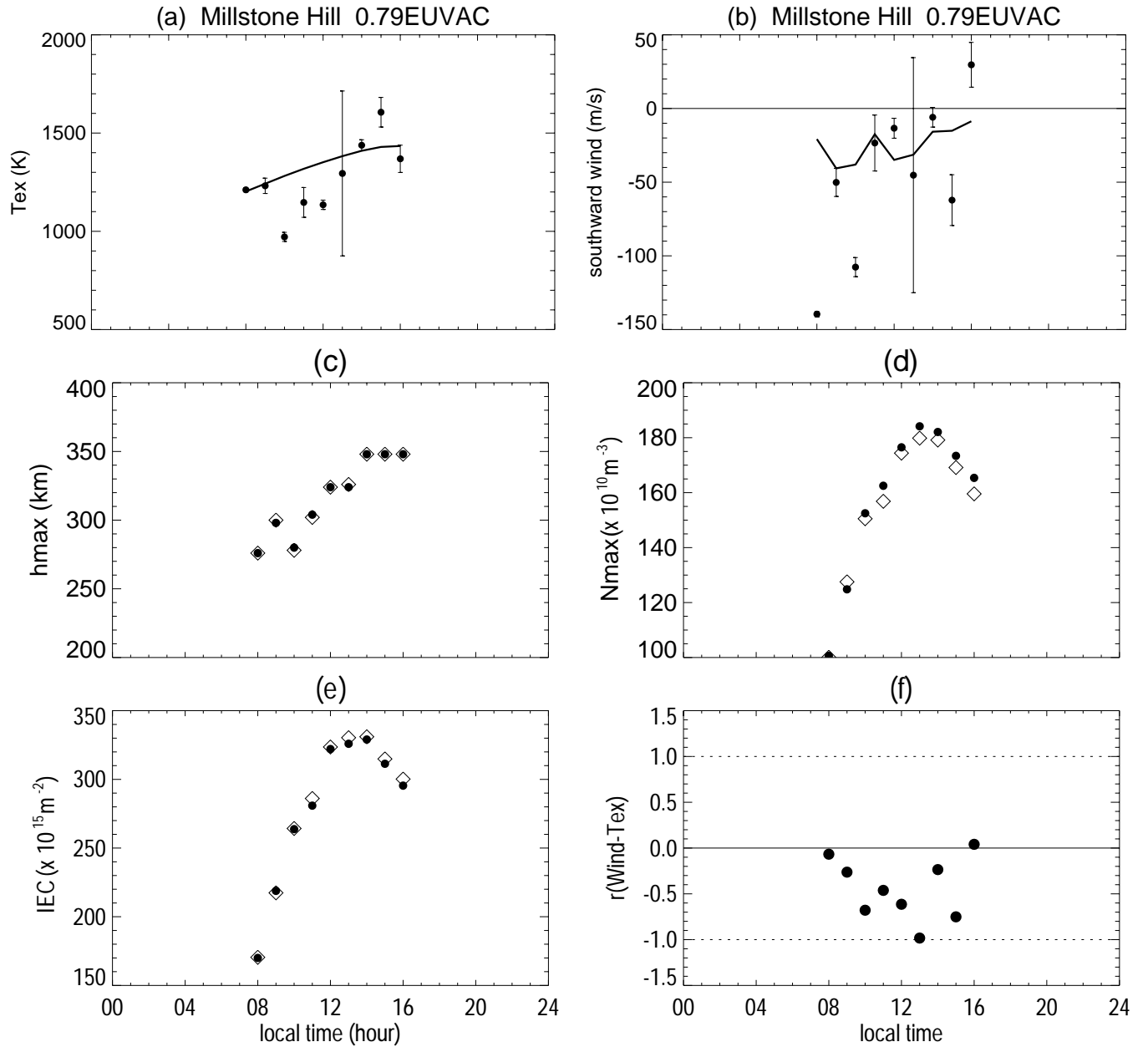


Figure 2. Assimilation results with N_{max} - h_{max} -IEC data set for Millstone Hill and EUV flux is 0.79 times the default model values. (a) The inferred T_{ex} (dots and error bars; the solid line is for MSIS model), (b) the inferred southward wind (dots and error bars; the solid line is the default model values of horizontal wind model(HWM)-like model for MU radar (HWMU)), (c) original h_{max} data (diamonds) and fitted values (dots), (d) original N_{max} data (diamonds) and fitted values (dots), (e) original IEC data (diamonds) and fitted values (dots), (f) Wind- T_{ex} correlation coefficient.

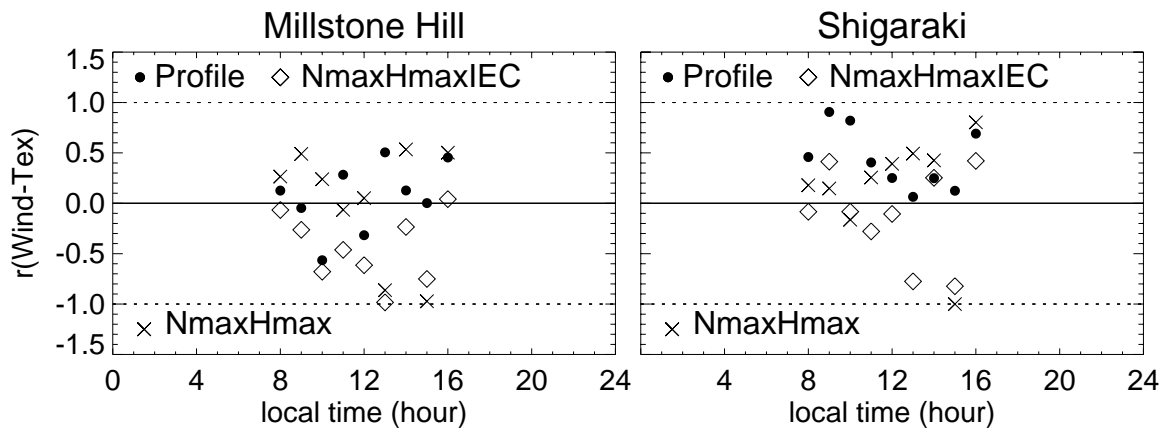


Figure 3. The uniqueness of the inferred wind and T_{ex} indicated by their correlation coefficient for Millstone Hill and Shigaraki. Dots are obtained with the profile assimilation, diamonds with N_{max} - h_{max} -IEC data, and crosses with N_{max} - h_{max} data.

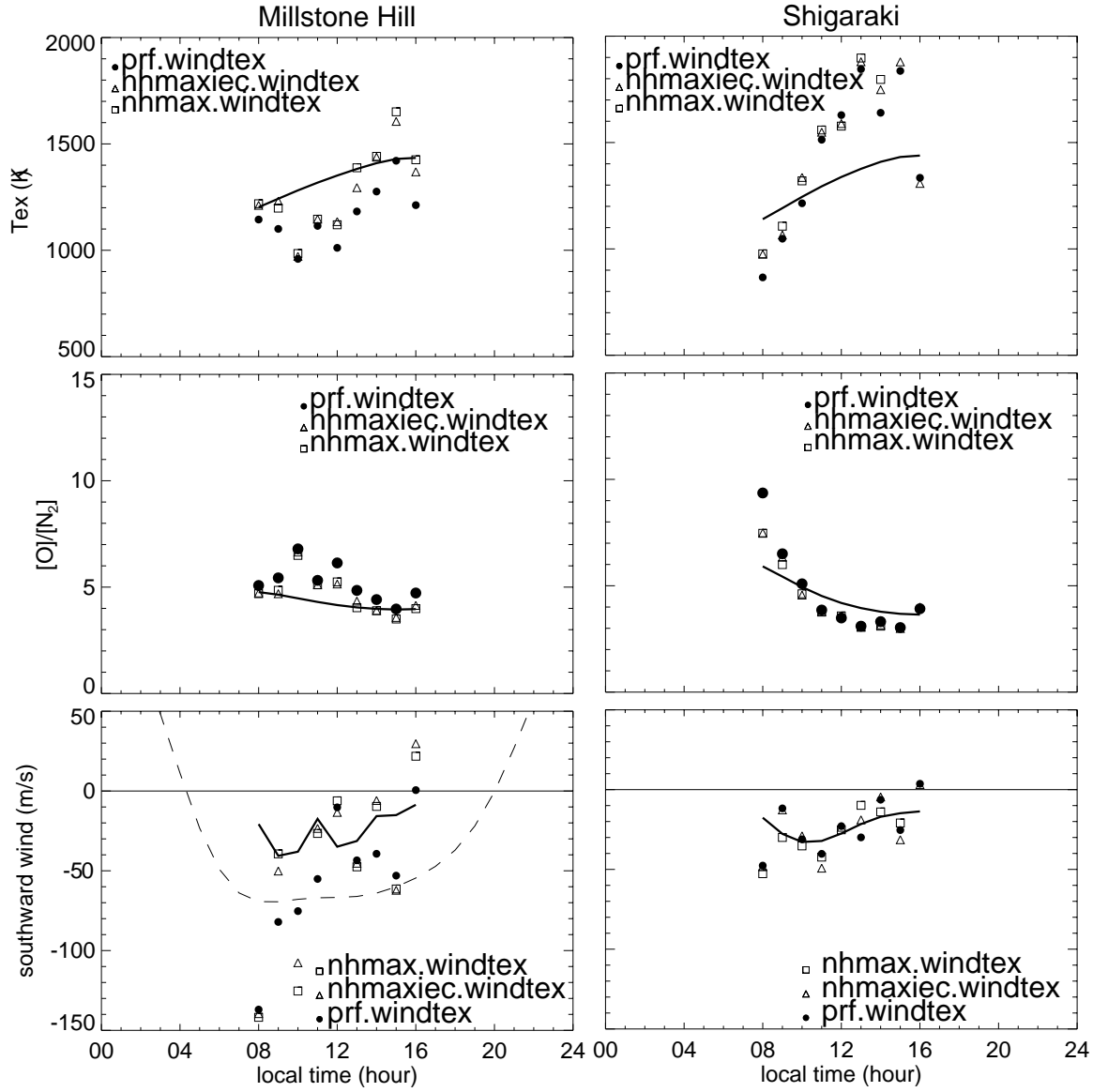


Figure 4. Comparisons of inferred variables for different assimilation data. Left panels are for Millstone Hill and right panels for Shigaraki. Top panels are for T_{ex} , middle panels for 300-km $[O]/[N_2]$ ratio calculated with the the mass spectrometer and incoherent scatter (MSIS86) model for the inferred T_{ex} , and bottom panels are for southward winds. Dots are obtained with the profile data assimilation, triangles with N_{max} - h_{max} -IEC data, squares with N_{max} - h_{max} data. Solid lines in the top and middle panels are for the MSIS model values, in the bottom panels they are ion drift-based wind measurements for the left panel, and HWMMU model values for the right panel.

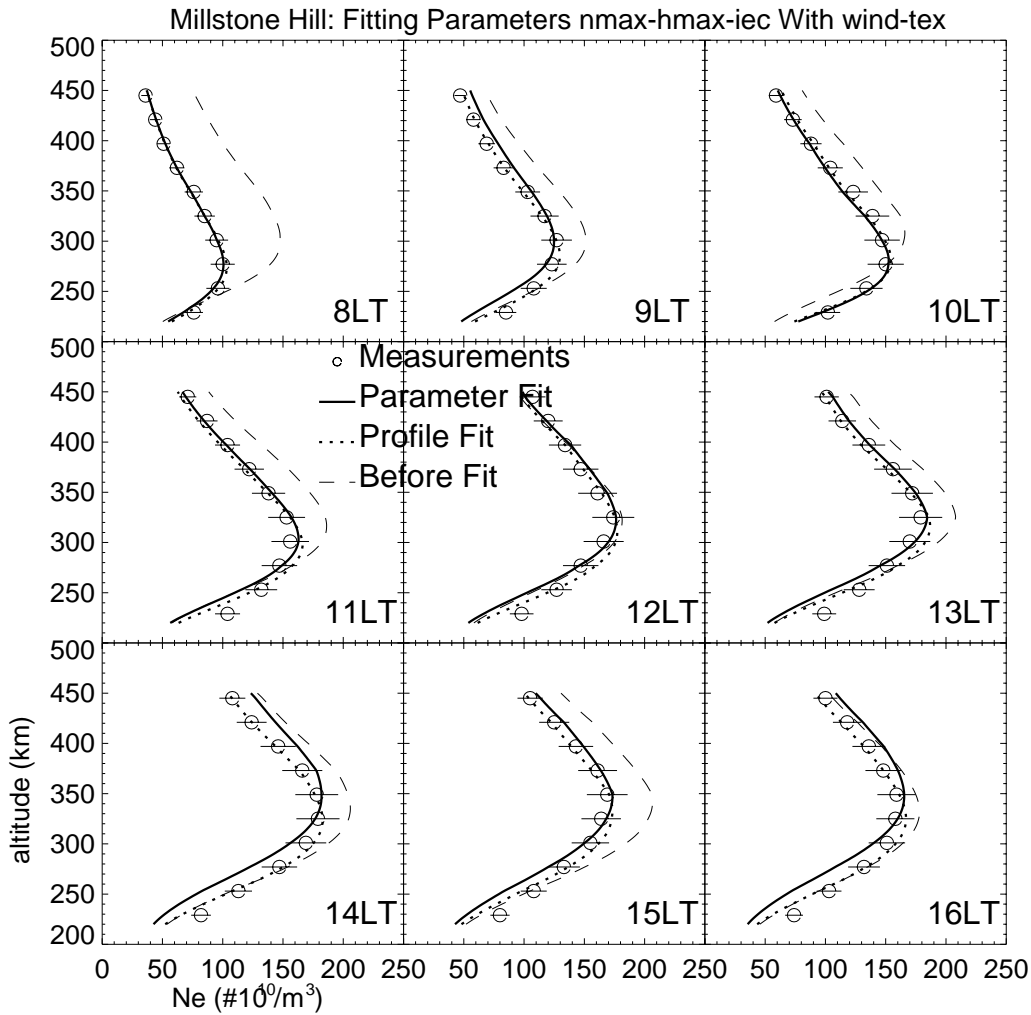


Figure 5. Profile comparisons for Millstone Hill at each hour from 0800 LT to 1600 LT. Circles are for measurements (the error bars is an assumed 10% uncertainty for the data), solid lines are the best matched model profile from the profile data assimilation, and dashed lines are the best matched model profile from N_{max} - h_{max} -IEC data assimilation.

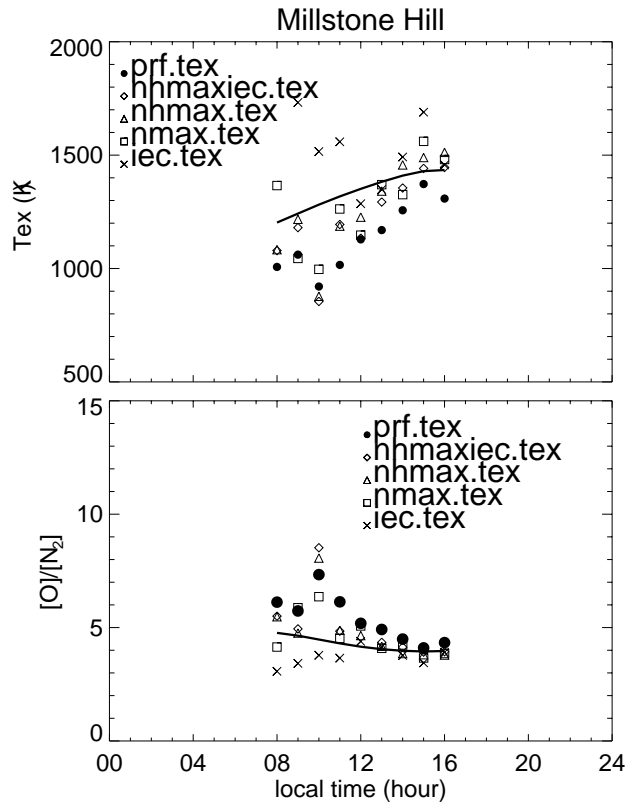


Figure 6. Comparisons of the inferred T_{ex} and $[O]/[N_2]$ for different assimilation data over Millstone Hill. The top panel is for T_{ex} and the middle panel for 300-km $[O]/[N_2]$ ratio calculated with MSIS86 model for the inferred T_{ex} . Dots are obtained with the profile data assimilation, diamonds with N_{max} - h_{max} -IEC data, triangles with N_{max} - h_{max} data, squares with N_{max} data, and crosses with IEC data. Solid lines are for the MSIS model values

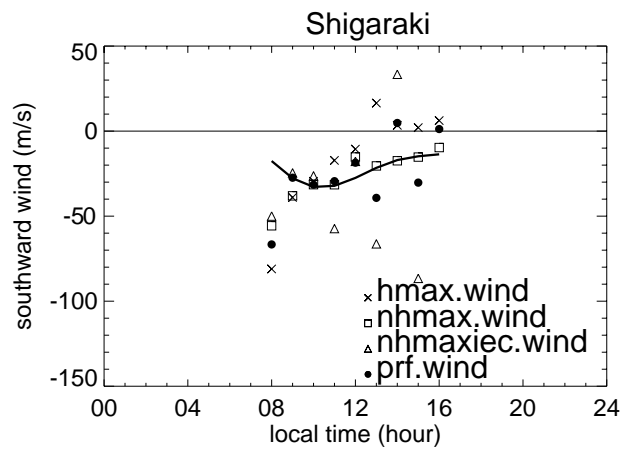


Figure 7. Comparisons of the inferred southward winds for different assimilation data over Shigaraki. Dots are obtained with the profile data assimilation, triangles with N_{max} - h_{max} -IEC data, squares with N_{max} - h_{max} data, and crosses with h_{max} data. The solid line is for HWMMU model values.